Sustainable LightAssisted 3D Printing of BioBased MicrowaveFunctionalized Gallic Acid

Macromolecular Chemistry and Physics
www.mcp-journal.de

Sustainable Light-Assisted 3D Printing of Bio-Based Microwave-Functionalized Gallic Acid

*Rossella Sesia, Matilde Porcarello, Minna Hakkarainen, Sara Ferraris, Silvia Spriano, and Marco Sangermano**

The development of 3D printing technologies and the requirement for more sustainable 3D printing materials is constantly growing. However, ensuring both sustainability and performance of the new materials is crucial to replace current fossil-based polymers. Here, a bio-based UV-curable resin is produced in high yield from gallic acid (GA), a natural polyphenolic compound, by means of rapid and efficient microwave-assisted methacrylation (5 min heating time and 10 min at 130 °C). The successful microwave-assisted methacrylation with a high degree of substitution is confirmed by Fourier transform infrared (FTIR) spectroscopy and proton nuclear magnetic resonance spectroscopy. The radical UV-photopolymerization of the methacrylated gallic acid (MGA) is further investigated by real-time FTIR and differential scanning photo calorimetry (photo-DSC) analyses, clearly demonstrating the high photo-reactivity of MGA. Moreover, the %gel assessment demonstrates the formation of highly insoluble fractions after the UV-curing, with 98% gel content. The photo-rheology and rheology support the suitability of MGA for light-assisted 3D printing. Indeed, a honeycomb and a hollow cube are 3D printed by means of the digital light processing 3D printing technique with high accuracy in a small scale. Finally, the cured-MGA illustrates high T_g and thermal stability.

1. Introduction

Additive manufacturing has rapidly spread as an innovative production method in scientific research and industrial fields. Unlike traditional processes, which imply materials and energy waste, 3D printing can produce objects in layer-by-layer fashion according to 3D drawings.[1–3] The potential advantages of 3D printing, such as free design, accurate resolution, quick execution time, and material savings, explain its outstanding success.[4,5] Among the various 3D printing techniques, light-assisted approaches, such as stereolithography (SL) and digital light processing (DLP), have gained much attention.[6–10] In particular, DLP printing is a vat photopolymerization technique, which offers a good combination of high resolution (≈1 m) and quick printing speed ($mm^3\ S^{-1}$).[4,11] Since DLP printing exploits a digital projector as a UV light source to induce polymerization, a reactive and easily amenable to photo-crosslinking DLP resin is needed. (Meth)acrylated monomers and oligomers have proven to be exploitable for 3D printing due to their high reactivity and faster reaction rates toward radical photopolymerization.[12,13] However, most of the photosensitive materials compatible with DLP are based on fossil resources and not produced in a sustainable way.[14,15]

In the green chemistry and sustainability framework, the development of polymeric materials from bio-renewable and biodegradable sources has become a demanding need to reduce the exploitation of fossil resources, CO_2 emission, and plastic waste. Therefore, the development of materials from different biomass resources, especially by utilizing waste and side-products from, for example, forest and food industry and agriculture, has gained widespread attention due to abundant availability, ease of extraction, non-toxicity, biodegradability, and low cost. Among biomass-based monomers, oligomers, or polymers for 3D printing, many compounds functionalized with photocurable groups, including cellulose, lignin, chitosan, polylactide acid, and natural oils, have been investigated.[5,12,16–26]

To date, surprisingly limited attention has been paid to natural polyphenolic compounds. The class of polyphenols consists of numerous molecules, that are ubiquitous in the plant world and can be extracted for innumerable application purposes.[27–35] Gallic acid (GA), also known as 3,4,5-trihydroxybenoic acid, is a polyphenolic compound classified as phenolic acid. It can be found freely in plants or obtained from hydrolysis of gallotannins, such as tannic acid, present in nature.[30,36–39] Since the chemical structure shows multiple active sites, including

R. Sesia, M. Porcarello, S. Ferraris, S. Spriano, M. Sangermano
Dipartimento Scienza Applicata e Tecnologia
Politecnico di Torino
Corso Duca degli Abruzzi 24, Torino 10129, Italy
E-mail: marco.sangermano@polito.it
M. Hakkarainen
Division of Polymer Technology
Department of Fibre and Polymer Technology
KTH Royal Institute of Technology
Teknikringen 56-58, Stockholm SE-100 44, Sweden
The ORCID identification number(s) for the author(s) of this article can be found under https://doi.org/10.1002/macp.202400181

DOI: 10.1002/macp.202400181

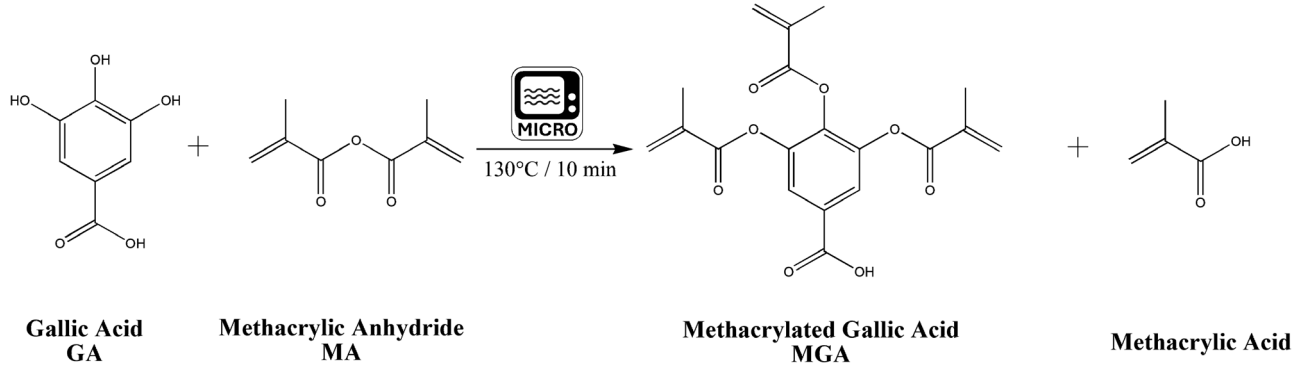

Scheme 1. Schematization of the microwave-assisted methacrylation reaction of gallic acid (GA) by methacrylic anhydride (MA). The reaction produces methacrylated gallic acid (MGA) and methacrylic acid as a by-product.

pyrogallic groups (three hydroxyl groups) and a rigid benzene ring, GA is of high interest for the production of high-performance thermosetting materials.[40–45] Zhu et al. investigated GA as a thermo-mechanical reinforcing agent in oil-based 3D printing materials. For this purpose, the chemical modification of GA was necessary. Hence, Zhu at al. synthetized the methacrylated gallic acid (MGA) to incorporate a high number of hydrophobic and reactive C═C functionalities in GA.[46] However, the one pot method used to obtain MGA was very long and exploited dangerous chemicals for human health and environmentally toxic reagents, such as 4-dimethylaminopyridine, triphenylphosphine, and hydroquinone.[47–51]

Microwave irradiation is an outstanding competitive eco-friendly alternative to traditional heating functionalization methods. Indeed, it ensures fast, volumetric, and selective heating through the excitation of polar molecules. Therefore, microwave-assisted processes enable more efficient energy transfer.[52–54] In addition, microwave irradiation typically leads to higher yields and improved purity for the products achieved under milder experiment conditions and significantly reduced reaction times.[55–58]

In the present work, we propose a microwave-assisted rapid methacrylic functionalization to produce UV-curable MGA monomer without the need for additional solvents or catalysts. Moreover, the 3D printability of MGA and the thermal properties of 3D-printed materials were evaluated.

2. Results and Discussion

2.1. Microwave-Assisted Methacrylation Reaction of Gallic Acid

The potential of microwave-assisted functionalization of gallic acid (GA) was exploited to introduce the UV-curable methacrylate moieties. The covalent grafting of methacrylate functionalities has been proved an efficient strategy to obtain a photoreactive resin for additive manufacturing via digital light processing (DLP).[58,59] The polyphenolic active sites of GA have been demonstrated suitable as chemical handles for the methacrylation reaction.[46]

In this study, GA was methacrylated through microwave-assisted functionalization (**Scheme 1**) based on previous works on methacrylation and acetylation of lignin, which found out the optimal reaction parameters to maximize the product yield and the substitution degree of phenolic compounds.[59,60] No previous studies have investigated the microwave-assisted methacrylation reaction of polyphenols, in particular phenolic acids like gallic acid. Through this solvent-free and catalyst-free methacrylation method, significantly reduced reaction time (10 min) and moderate reaction temperature (130 °C) were used to achieve a yield of the methacrylated gallic acid (MGA) ≈90%.

The successful methacrylation of GA via microwave-assisted reaction was investigated by FTIR analysis (**Figure 1**). The appearance of the signal at 1740 cm^{-1}, assigned to C═O stretching vibrations in phenolic esters and the peak of C═C stretches at 1633 cm^{-1}, supports the presence of methacrylate groups in MGA. Moreover, in the MGA spectrum the new peak at 945 cm^{-1}, corresponding to the in-plane C═CH_2 bend, assured the effective functionalization. Finally, the decrease in intensity of the OH band (3600–3000 cm^{-1}) confirmed the consumption of phenolic groups due to the methacrylation reaction.

Finally, the characterization of GA and MGA by proton nuclear magnetic resonance (^{1}H NMR) spectroscopy further confirmed the methacrylation functionalization. **Figure 2a** shows the ^{1}H NMR spectrum of pristine GA with its characteristic peaks

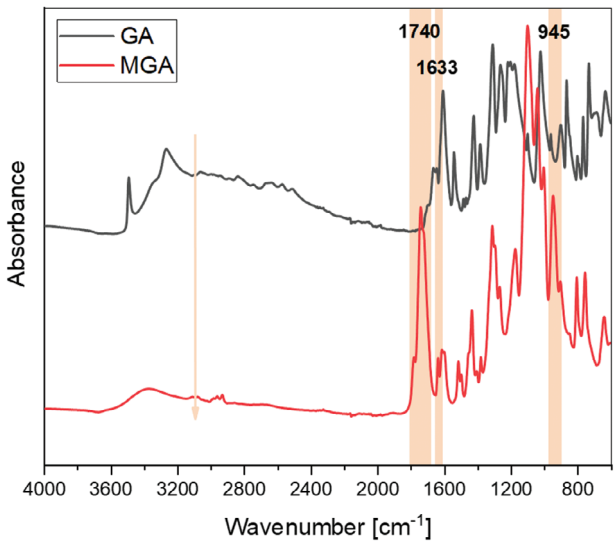

Figure 1. ATR-FTIR spectra of GA (black line) and MGA (red line).

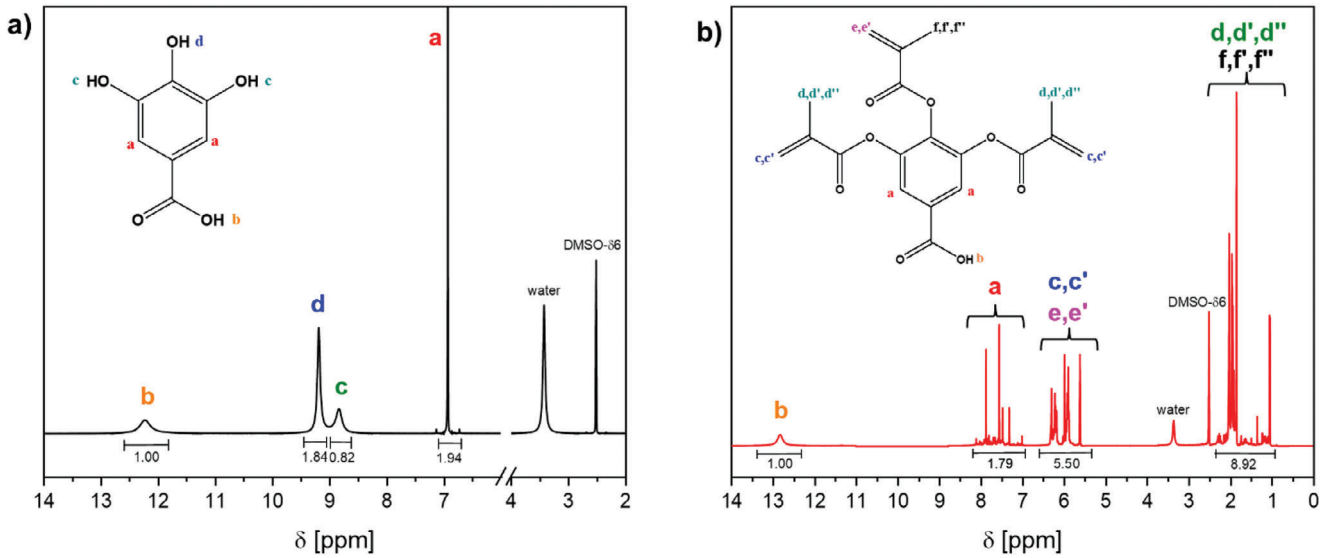

Figure 2. ^{1}H NMR spectra of a) gallic acid (on the left, black line) and b) methacrylated gallic acid (on the right, red line).

corresponding to the hydroxyl-hydrogens, named c and d. Instead, after the microwave-assisted methacrylation reaction the observed disappearance of these peaks assigned to phenolic hydroxyl groups can be explained by the introduction of methacrylate moieties, which is further supported by the spectrum of MGA seen in Figure 2b. The several multiplets in the MGA ^{1}H NMR spectrum were generated by the various possible geometric isomers of the double bond hydrogens. Moreover, from the ^{1}H NMR analysis, it is evident that the peak b related to the hydrogen in the carboxylic group was not affected by the functionalization. Therefore, the structural characterization of MGA by ^{1}H NMR spectroscopy fully supported the successful microwave-assisted methacrylation.

2.2. Photocrosslinking Investigation

The photopolymerization process of MGA was investigated by means of real-time FTIR, photo-DSC, and photo rheology. By means of real-time FTIR, the conversion of photoreactive groups into MGA was monitored as a function of UV light irradiation time. **Figure 3** reports the spectra of MGA formulation before the UV-curing and after 180 s of light irradiation. As can be seen, the intensity of the signal at 1633 cm^{-1} related to C═C stretches decreased with the irradiation time because of the radical photopolymerization, as well as the area of the peak at 945 cm^{-1}.

Conversion curves as a function of irradiation time were calculated following the decrease of the area of the peak at 1633 cm^{-1}, which provides an indication of the effectiveness of the photocuring process. The effect of the radical photoinitiator concentration in the photocurable formulation on the UV-curing rate and the final MGA conversion was evaluated (**Figure 4**).

What stands out, in the conversion degree plot, is the increase in the final conversion as the BAPO's concentration increases, as also **Table 1** reports. The increased concentration of photoinitiator and consequently of radicals, which are produced during irradiation, could explain this observation. Indeed, higher amounts of photogenerated radicals were available to initiate the MGA's crosslinking, resulting in faster kinetics and a higher degree of conversion.[61] The complete conversion for all three MGA formulations was achieved after 180 s of UV light irradiation with values in a range between 80 and 90%.

Therefore, real-time FTIR data reported here affirm the good reactivity to UV light of MGA, synthesized via microwave-assisted functionalization. However, contrary to expectations, the MGA formulation with 2 phr of BAPO was found to be more effective, after 180 s of irradiation, than the formulation containing 3 phr of BAPO (Table 1). This result can be explained by the competitive effect on the growth of the polymeric chains due to the higher amount of photoinitiator radicals.[62] Indeed, in MTA formulation with 3 phr of BAPO, the coupling between the photogenerated radicals from the photoinitiator occurred, preventing the homolytic cleavage of the methacrylic double bond. As a result, a slight decrease in the final conversion was achieved due to an inner filter effect.

The gallic acid-based resin developed by G. Zhu et al. reached a similar double bond conversion ranging from 83% to 91% in 10 min.[46] In addition, R. Ding et al. confirmed the rapid photocuring kinetic of natural phenolic-based methacrylates and evaluated a C═C conversion of 88.5–99.4% after 60 s of irradiation.[63]

In order to validate the real-time FTIR data, photo-DSC experiments were carried out on the same MGA formulations and under the same temperature curing conditions, that is, 25 °C. This analysis revealed a few crucial factors: the time at the maximum rate of polymerization (t_{peak}), the peak height at the maximum of the DSC curve (h_{peak}), and the heat release (ΔH), assessed as the total enthalpy from the curing peak integration (**Table 2**). **Figure 5** collects the photo-DSC curves for the MGA formulations with different BAPO concentrations with the aim of investigating the photoinitiator effect by the curing peak evaluation. As it can be noticed, the lowest t_{peak} was measured for the BAPO content of 2 phr, which implied a fast photocrosslinking process.

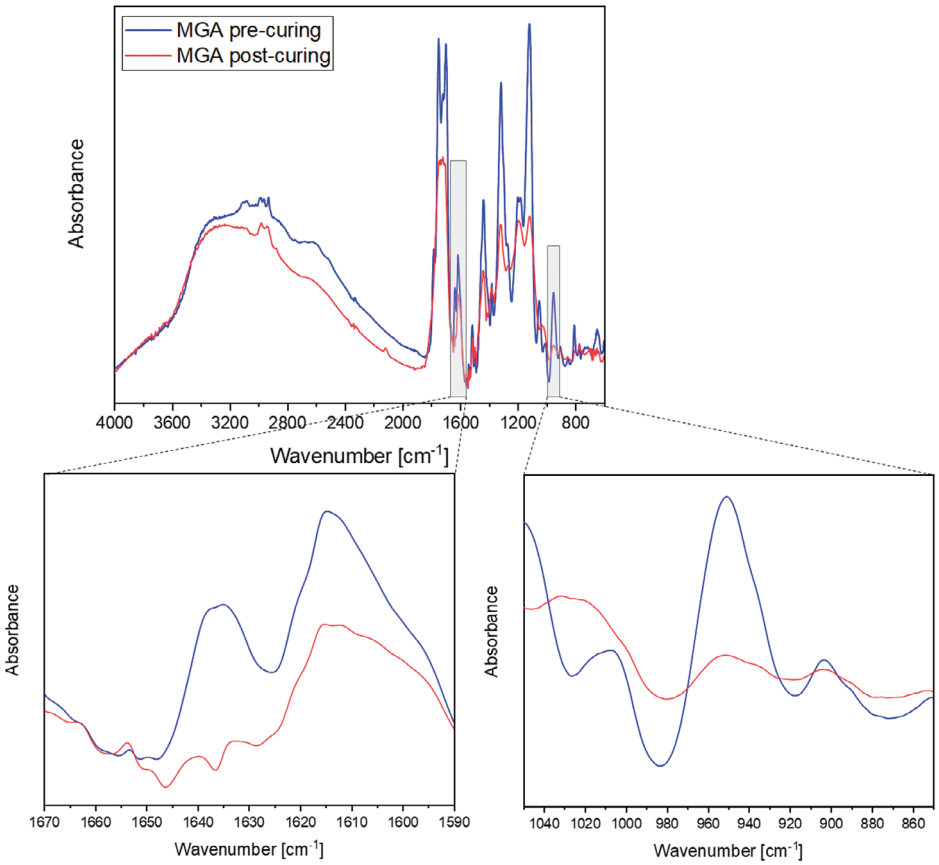

Figure 3. Real-time FTIR spectra of MGA formulation with 2 phr of BAPO photoinitiator before (pre-curing, blue line) and after (post-curing, red line) UV light irradiation.

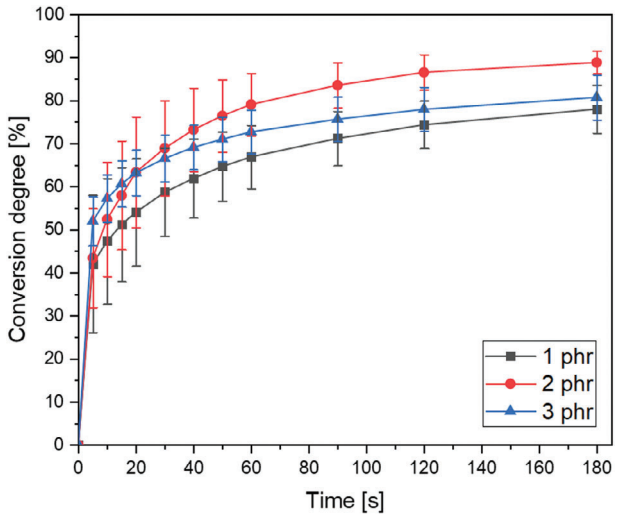

Figure 4. Conversion degree of C=C methacrylate groups as a function of irradiation time for MGA with 1 phr (black line), 2 phr (red line), and 3 phr (blue line) of BAPO.

Overall, taking into consideration the standard deviations, no significant variations were recorded on the measured parameters between the three different contents of the photoinitiator, demonstrating the high photo-reactivity of MGA, noted by real-time FTIR experiments.

Therefore, from the results of the real-time FTIR and photo-DSC analyses, the addition of 2 phr of the radical photoinitiator to MGA formulation was chosen for the subsequent experiments and DLP 3D printing, as it led to high double bond conversion degree and photocuring rate.

In order to investigate the gel fraction after the photopolymerization and assess the organic solvent resistance, the gel content (%gel) was evaluated on UV-cured MGA after 24 h of extraction in chloroform, and the MGA-based polymer showed a %gel of 98% ± 0.2. The high %gel value of UV-cured MGA was in accordance with the high conversion degree and demonstrated the effective formation of insoluble fraction due to the crosslinks between the MGA polymeric chains.

The last investigation of the photocuring process was performed through photo-rheological tests. The gelification time (t_{gel}), which occurs when the storage modulus (G') and the loss modulus (G'') are equal, was determined. In **Figure 6**, the curve of the measurement is represented, where it is possible to observe that the MGA reacts almost immediately. This is underlined by the steep increase of the moduli during the first 20 s after the UV lamp activation, reaching the t_{gel} after 5 s which makes it appropriate for the 3D printing process.

In addition, rheological measurements were carried out on MGA, with particular attention on the range of interest for DLP

Table 1. Conversion degrees, calculated by Equation (1), for MGA formulations with different BAPO's contents after a certain time of UV light irradiation.

BAPO concentration	Conversion degree [%] after 5 s	Conversion degree [%] after 30 s	Conversion degree [%] after 60 s	Conversion degree [%] after 180 s
1 phr	42 ± 16	59 ± 10	67 ± 7	78 ± 6
2 phr	43 ± 11	69 ± 11	79 ± 7	89 ± 3
3 phr	52 ± 6	66 ± 5	73 ± 5	81 ± 5

Table 2. Photo-DSC results of MGA formulations with different BAPO's concentrations.

BAPO concentration	t_{peak} [s]	h_{peak} [W g^{-1}]	ΔH [J g^{-1}]
1 phr	4.7 ± 0.6	30.2 ± 6.2	231.5 ± 3.2
2 phr	4.7 ± 0.6	29.2 ± 5.7	225.7 ± 14.5
3 phr	5.3 ± 1.2	22.3 ± 4.0	229.7 ± 17.4

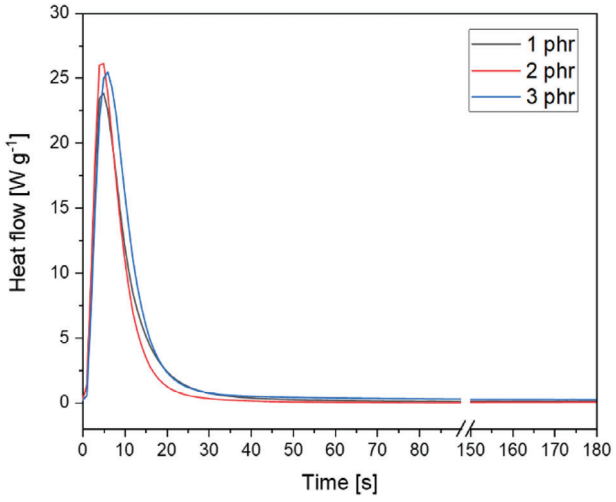

Figure 5. Photo-DSC thermograms for MGA formulations with 1 phr (black line), 2 phr (red line), and 3 phr (blue line) of BAPO.

3D printing (**Figure 7**).[64] MGA showed shear thinning behavior in the range of shear rate considered with the viscosity that linearly decreases when shear rate values increase. This behavior is acceptable for 3D printing since the viscosity decreases and remains inside the range of shear rate applied during DLP 3D printing.

2.3. Thermal Characterization of UV-Cured MGA

The glass transition temperature (T_g) of the photocrosslinked MGA was assessed by means of DSC analysis. As observed in **Figure 8a**, the MGA-based polymer showed a T_g of 122 °C. This high T_g denotes chain mobility restrictions, and indicates a significant crosslinking density. This value is comparable with the T_g of gallic acid-based resin studied by G. Zhu et al. (118–130 °C).[46] Moreover, the estimated T_g of MGA proved to be higher than photocured other natural phenols-based methacrylates, as demonstrated by the values ranging from 45 to 107.5 °C measured by R. Ding et al.,[63] and the T_g of ≈56–75 °C for vanillin thermosets.[65,66] In addition, UV-cured resin based on methacrylated eugenol and vanillin alcohol with methacrylated lignin filler showed significantly lower values (28–45 °C) than UV-cured MGA.[59]

The thermal stability of UV-cured MGA was studied by TGA experiments in an inert atmosphere. The TGA thermogram showed a two-step degradation profile (Figure 8b). The first step (170–315 °C) could indicate decomposition of not completely cured MGA, such as dangling chain ends. Instead, the random scission of crosslinked chains and the phenolic moieties degradation are likely responsible for the second stage (315–460 °C) occurring at significantly high temperatures.[59,67,68] The measured char yield (w_{char}) was ≈16% and the thermal degradation temperature of 20% mass loss ($T_{deg20\%}$) was ≈277 °C, implying a high thermal stability due to the high crosslinking density and aromatic content. This result also accords with the previous degradation temperature measured on methacrylated gallic acid-based polymer and natural phenolic methacrylates, implying thermal stability below 300 °C.[46,63]

2.4. 3D Printing

Taking into account the promising results of rheological tests, DLP 3D printing of the MGA formulation was carried out. Two different complex structures were printed to demonstrate the 3D printability of MGA. The first one was a honeycomb with a total volume of 10 × 10 × 1 mm, while the second one was a hollow cube with a total volume of 5 × 5 × 5 mm and a wall thickness of 0.8 mm. The CAD models and some pictures of the honeycomb and the hollow cube are presented in **Figures 9** and **10**, respectively.

As it is possible to state from Figures 9 and 10, the printing process with MGA is very accurate in small-scale objects. Indeed, the thickness of the walls of the hexagonal cells is well defined considering its thickness of 0.5 mm, as can be seen from the stereo microscopy magnification (Figure 9b**)**. On the other hand, printing the hollow cube demonstrated the capability to also produce taller, slender structures while maintaining their thinness (e.g., 0.8 mm as shown in Figure 10a). Hence, it is possible to conclude that MGA formulations are appropriate as resins for the 3D printing process.

3. Conclusion

Gallic acid (GA) from natural resources was successfully methacrylated by methacrylic anhydride and microwave-assisted reaction. This functionalization process allowed to produce a

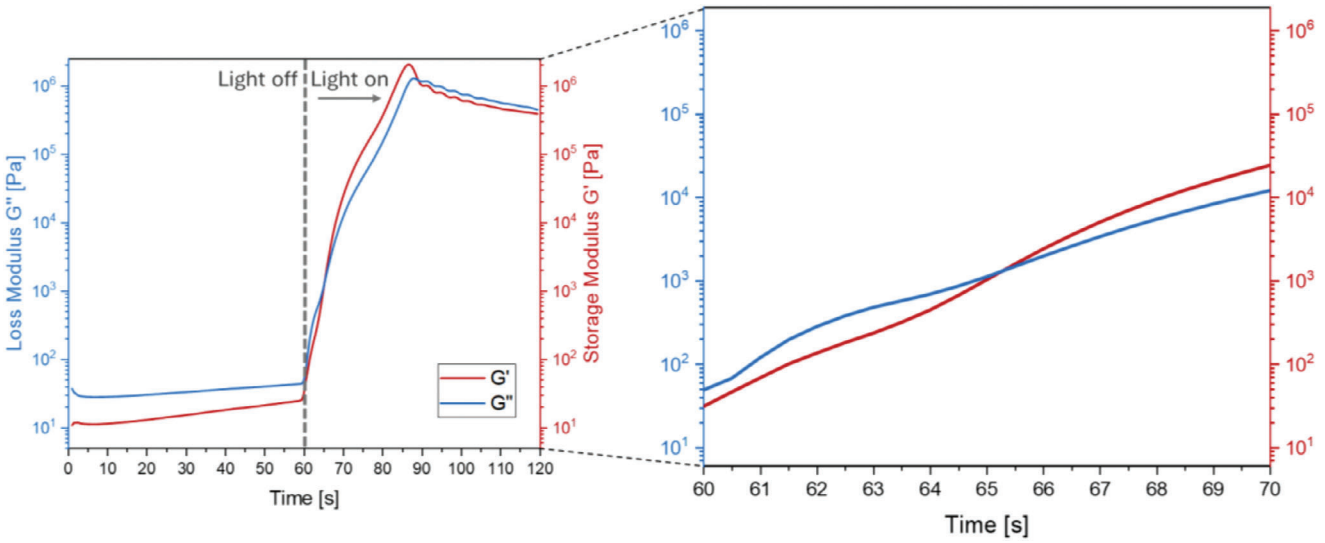

Figure 6. Photorheological curve of MGA formulation with 2 phr of BAPO with the highlight of t_{gel}.

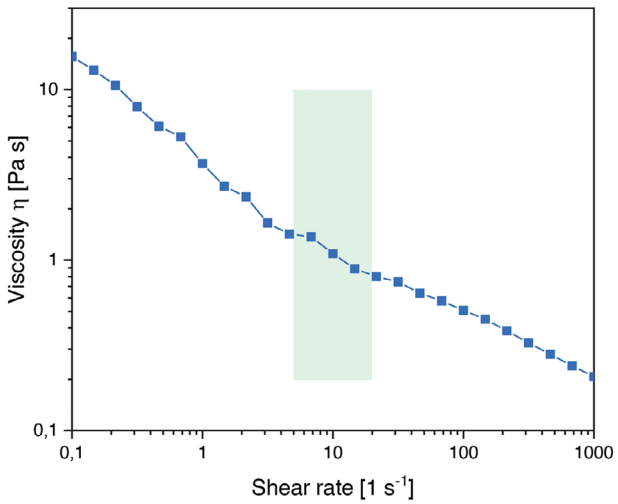

Figure 7. Viscosity curve of MGA formulation with 2 phr of BAPO.

3D printable bio-based resins without additional solvents and catalysts in short reaction times. The successful methacrylation of GA to produce MGA, in high-yield and high degree of substitution, was confirmed by FTIR and ^{1}H NMR analyses.

The radical photocrosslinking process of MGA and the influence of photoinitiator concentration on the conversion degree were assessed by real-time FTIR spectroscopy. Around 90% conversion degree in the MGA formulation with 2 phr of photoinitiator was reached after 180 s of UV light irradiation, thus identifying this photoinitiator content as suitable for 3D printing. Moreover, photo-DSC analysis corroborated the high photo-reactivity of MGA. The results of gel content analysis proved the high insoluble fraction due to the effective crosslinking of UV-cured MGA's chains. In order to evaluate the possibility of 3D printing MGA formulation, photo-rheology and rheology were performed. Photo-rheological measurements confirmed the immediacy of MGA UV-curing with a t_{gel} after 5 s, while the MGA's rheological behavior was assessed inside the range of shear rate applied in the 3D printing process. Furthermore, MGA had a high T_g of ≈122 °C and high thermal stability.

Finally, the possibility to exploit the methacrylate moieties in the eco-friendly MGA for 3D printing through the DLP technique was proven. Two objects with different structures were 3D printed: a honeycomb and a hollow cube. Both the MGA-based objects showed an outstanding accuracy in a small scale, as further supported by the stereo microscope magnification pictures. Moreover, the possibility to 3D print taller and slighter structures was proven by the hollow cube. The evidence from this study indicates a high potential for the production of sustainable 3D printable natural polyphenols-based resins.

4. Experimental Section

Materials: Gallic acid (GA) and methacrylic anhydride with purity of 94% (MA, inhibited with 2.000 ppm topanol A) were purchased from Sigma Aldrich. Acrylated epoxidized soybean oil (AESO, inhibited with 4.000 ppm monomethyl ether hydroquinone) and isobornyl acrylate (IBOA, with 200 ppm monomethyl ether hydroquinone as inhibitor) were purchased from Sigma Aldrich, as well as phenylbis(2,4,6-trimethylbenzoyl)phosphine oxide (BAPO) and dimethylsulfoxide-d6 (DMSO-d6, purity of 99.8%). Finally, chloroform (≥99.8%, with 0.5–1.0% of ethanol as a stabilizer), and isopropanol (≥99.5%) were obtained from Sigma Aldrich. All chemicals were used as received and without further purification.

Synthesis of Methacrylated Gallic Acid (MGA): Gallic acid (GA) was methacrylated, using microwave-assisted technology, according to a procedure adapted from previous works.[13,59,60] GA and methacrylic anhydride (MA) were introduced to 100 mL high-pressure Teflon vessels at a weight ratio of 1:5 GA to MA and thoroughly mixed. The vessel was exposed to microwave irradiation (flexiWAVE MA186-001 microwave) for isothermal heating at 130 °C for 10 min. A ramp time of 5 min and a maximum power of 1200 W were settled. Afterward, the vessel was cooled to room temperature with a cooling time of 10 min. Subsequently, the vessel content was poured into distilled water to precipitate the methacrylated gallic acid (MGA). The obtained suspension was stirred for 24 h at room

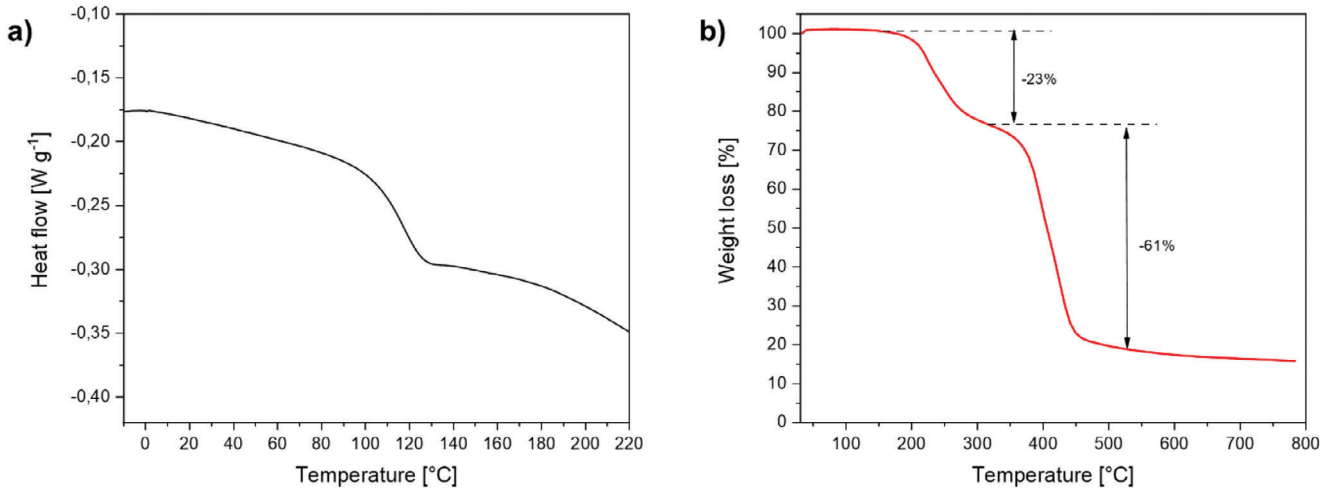

Figure 8. On the left a) the DSC curve and on the right b) the TGA thermogram of UV-cured MGA.

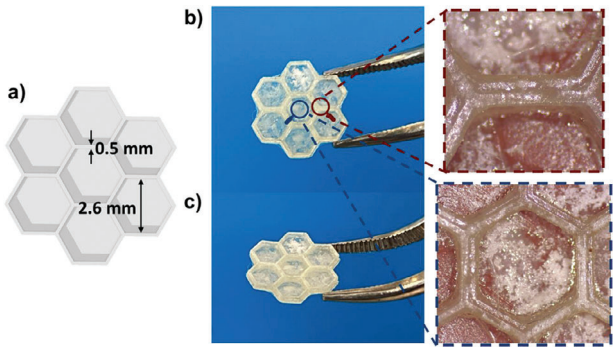

Figure 9. a) CAD model of the honeycomb with cell measures; b) and c) images of the printed object with stereo microscope magnification pictures of the details.

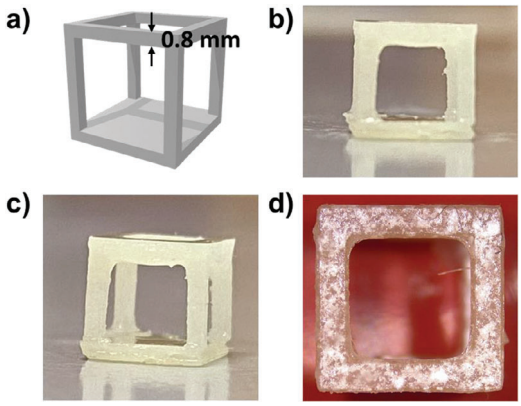

Figure 10. a) CAD model of the hollow cube with wall thickness measure; images of the printed object b) from the frontal and c) lateral point of view; d) stereo microscope magnification picture of the top view of the cube.

temperature and then vacuum filtrated. Finally, MGA was dried under vacuum at room temperature for at least 48 h.

^{1}H NMR of GA (400 MHz, DMSO-d_6, δ): 12.23 (s, 1H, COOH),9.21–9.16 (m, 2H, OH), 8.84 (s, 1H, OH), 6.93 (s, 2H, Ar H).

^{1}H NMR of MGA (400 MHz, DMSO-d_6, δ): 12.83 (s, 1H, COOH), 8.19–6.89 (m, 2H, Ar H), 6.77–5.13 (m, 6H, C = CH_2), 2.34–0.61 (m, 9H, CH_3).

Characterization Methods: Nuclear magnetic resonance (NMR) spectroscopy – The synthesized MGA was characterized by proton nuclear magnetic resonance (^{1}H NMR) spectroscopy at 400 MHz and 25 °C, utilizing a Bruker Avance 400 spectrometer. Dimethylsulfoxide-d6 (DMSO-d6) was used as the solvent and the internal standard for calibrating the chemical shift.

Fourier transform infrared (FTIR) spectroscopy – In order to investigate the structural changes before and after the methacrylation reaction, a PerkinElmer Spectrum 100 instrument, in an attenuated total reflection (ATR) mode, equipped with a diamond crystal was used. The ATR-FTIR spectra were acquired with a resolution of 4 cm−^{1} and resulted as average of 16 scans.

The photocrosslinking process was monitored by using a Thermo Scientific Nicolet iS50 FTIR spectrometer (Thermo Fisher Scientific, Milano, Italy). The concentration of BAPO photoinitiator mixed with the synthetized MGA was varied from 1 to 3 phr (per hundred resin). The liquid formulation was spread with a thickness of 12 µm on a silicon wafer by a film bar and irradiated by UV light under N_2 flow. A Hamamatsu LC8 lamp with an 8 mm light guide and spectral distribution range of 240–400 nm was used. The real-time FTIR spectra were collected in the range of 4000–600 cm^{-1} as 32 scans with a spectral resolution of 4.0 cm^{-1}. The conversion degree was evaluated by the disappearance of the C═C peak at 1633 cm^{-1}.[69–71] The C═O signal at 1780 cm^{-1} was taken as the reference, as it was assumed to be unaffected by UV light irradiation.[14,28] All measurements were performed as triplicate. The conversion degree was calculated according to the Equation (1).

$$Conversion\ [\%] = \frac{\left(\frac{A_{C=C}}{A_{C=O}}\right)_{t=0} - \left(\frac{A_{C=C}}{A_{C=O}}\right)_{t}}{\left(\frac{A_{C=C}}{A_{C=O}}\right)_{t=0}} \times 100 \quad (1)$$

where $A_{C=C}$ and $A_{C=O}$ are the areas of the methacrylic —CH═CH_2 stretches peak and the reference peak, respectively, evaluated at different times.

Differential scanning calorimetry (DSC) and photo-DSC – The UV-curing process was investigated through photo-DSC analysis. A Mettler Toledo DSC-1 instrument equipped with Gas Controller GC100 and a mercury lamp (Hamamatsu LightningcureTM LC8, Hamamatsu Photonics) with an optical fiber to directly irradiate the sample was used. The emission of UV light was centered at 365 nm and the lamp intensity was settled at 100%. To assess the influence of the BAPO's concentration (1, 2, and 3 phr) on the photopolymerization process, ≈5–10 mg of the UV-

curable liquid formulation was poured into an open 40 µL aluminum pan. An empty pan was taken as a reference. The measurements were carried out at room temperature (25 °C) under an N_2 atmosphere (flow rate of 40 mL min^{-1}). The samples were irradiated two times for 5 min. The second UV light exposure step was necessary to confirm the complete UV-curing and to create the baseline. The subtraction of the second curve from the first one allowed the obtainment of the curing curve.

All experiments were performed three times, and the data were analyzed by Mettler STARe software V9.2.

The assessment of the glass transition temperature (T_g) of photocured MGA was carried out by means of a Mettler Toledo DSC-1. The UV-cured sample (5–10 mg) was sealed in a 40 µL aluminum pan and covered with a pierced lid. The heating/cooling method was composed of three repeated heating-cooling cycles: first the sample was heated from −20–200 °C, then it was cooled to −20 °C; after that, the chamber was heated to 250 °C and subsequently again cooled to −20 °C; finally, the sample was heated until 300 °C. The experiments were performed with a heating/cooling rate of 10 K min^{-1} and under N_2 flow with a rate of 40 mL min^{-1}. The T_g was calculated from the third heating. All tests were performed in triplicate and the data were elaborated by Mettler STARe software V9.2.

Rheology and photo-rheology – Rheological and photo-rheological measurements were conducted with an Anton Paar Modular Compact Rheometer (Physica MCR 302, Graz, Austria) using plate–plate geometry with plates measuring 25 mm in diameter. The purpose of the analysis was to investigate the rheological behavior of the MGA and the UV-curing process to determine the printability of the formulation. During photo-rheological tests a Hamamatsu LC8 lamp (broad spectrum UV lamp centered at 365 nm) was employed as the light source (100 mW cm^{-2}). The lamp was positioned beneath the bottom plate (for this analysis a glass plate was used) and it was activated 60 s after the initiation of each test. The gap between the two plates was set at 0.6 mm and the shear frequency was maintained constant at 1 Hz. Viscosity measurements were conducted over a range of shear rates spanning from 0.01 to 1000 s^{-1}, with a separation gap between the plates of 1 mm. All the analyses were performed at room temperature and in triplicate to ensure the reliability and reproducibility of the results.

Gel content – The gel content percentage (%gel) was estimated on UV-cured MGA with 2 phr of photoinitiator by measuring the weight loss after 24 h of extraction with chloroform. About 100 mg of the sample was immersed in the solvent and then dried in air for a further 24 h. %gel was determined according to Equation (2).

$$\%gel = \frac{W_f}{W_i} \times 100 \quad (2)$$

where W_i and W_f are the weights of the dry sample before and after the treatment, respectively.

Thermogravimetric analysis (TGA) – TGA was performed by means of a Mettler–Toledo TGA 851e instrument (Mettler Toledo, Columbus, Ohio, USA). The sample was heated from 25 to 800 °C with a heating rate of 10 °C min^{-1} under 50 mL min^{-1} Ar flow. All curves were normalized to the unit weight of the samples.

3D Printing: 3D printing tests were conducted with digital light processing (DLP) 3D printer Asiga MAX UVX27 (Asiga, Australia) equipped with an LED source of 385 nm (*XY* pixel resolution of 27 µm while *Z*-axis resolution is 1–500 µm). Every printed layer was 50 µm in thickness, the light intensity was 50 mW cm^{-2}. To aid in the detachment of the object from the platform two layers made with AESO-IBOA formulation were created (both in weight percentage of 50, containing 1 phr of BAPO as photoinitiator). These two layers were irradiated for 1 s, then the printing process was interrupted to substitute the vat with AESO-IBOA formulation with the one containing MGA. MGA layers were irradiated for 2.5 s to avoid an overcuring phenomenon. The obtained object was then washed in isopropanol inside an ultrasonic bath for 3 min. The post-curing process was completed inside an Asiga Flash Cure UV lamp (Asiga, Australia) at 10 mW cm^{-2} for 3 min. Finally, magnification images of 3D printed objects were obtained by using a stereo microscope LEICA EZ4 W provided by Leica Microsystems (Wetzlar, Germany).

Acknowledgements

MUR for funding R. Sesia's Ph.D. fellowship (MUR–D.M.1061/2021–Dottorati di ricerca su tematiche green e dell'innovazione: nuove risorse dal PON Ricerca e Innovazione) and the European Union's Horizon 2020 research and innovation program under the Marie Skłodowska–Curie grant agreement, No 101085759 (SURE-Poly) are acknowledged. Silvateam S.p.A. is acknowledged for the collaboration, as well as Giovanna Colucci for TGA measurements. [Correction added on January 13, 2025, after first online publication: funding statement has been included in this version.]

Open access publishing facilitated by Politecnico di Torino, as part of the Wiley - CRUI-CARE agreement.

Conflict of Interest

The authors declare no conflict of interest.

Data Availability Statement

The data that support the findings of this study are available from the corresponding author upon reasonable request.

Keywords

3D printing, gallic acid, methacrylation, microwave irradiation

Received: June 9, 2024
Revised: July 4, 2024
Published online: July 15, 2024

[1] L. J. Tan, W. Zhu, K. Zhou, *Adv. Funct. Mater.* **2020**, *30*, 2003062.
[2] T. D. Ngo, A. Kashani, G. Imbalzano, K. T. Q. Nguyen, D. Hui, *Compos. B Eng.* **2018**, *143*, 172.
[3] G. N. Levy, R. Schindel, J. P. Kruth, *CIRP Ann.* **2003**, *52*, 589.
[4] G. Melilli, I. Carmagnola, C. TondaTuro, F. Pirri, G. Ciardelli, M. Sangermano, M. Hakkarainen, A. Chiappone, *Polymers* **2020**, *12*, 1655.
[5] M. Zanon, R. Cue-López, E. Martínez-Campos, P. Bosch, D. L. Versace, H. Hayek, N. Garino, C. F. Pirri, M. Sangermano, A. Chiappone, *Addit. Manuf.* **2023**, *69*, 103553.
[6] A. Bagheri, J. Jin, *ACS Appl. Polym. Mater.* **2019**, *1*, 593.
[7] R. Batchelor, T. Messer, M. Hippler, M. Wegener, C. Barner-Kowollik, E. Blasco, *Adv. Mater.* **2019**, *31*, 1904085.
[8] C. J. Thrasher, J. J. Schwartz, A. J. Boydston, *ACS Appl. Mater. Interfaces* **2017**, *9*, 39708.
[9] A. Cosola, R. Conti, H. Grützmacher, M. Sangermano, I. Roppolo, C. F. Pirri, A. Chiappone, *Macromol. Mater. Eng.* **2020**, *305*, 2000350.
[10] C. Dall'Argine, A. Hochwallner, N. Klikovits, R. Liska, J. Stampf, M. Sangermano, *Macromol. Mater. Eng.* **2020**, *305*, 2000325.
[11] W. Zhu, X. Ma, M. Gou, D. Mei, K. Zhang, S. Chen, *Curr. Opin. Biotechnol.* **2016**, *40*, 103.
[12] A. W. Bassett, A. E. Honnig, C. M. Breyta, I. C. Dunn, J. J. La Scala, J. F. Stanzione, *ACS Sustainable Chem. Eng.* **2020**, *8*, 5626.
[13] J. Yao, M. Hakkarainen, *Compos. Commun.* **2023**, *38*, 101506.
[14] M. Porcarello, S. Bonardd, G. Kortaberria, Y. Miyaji, K. Matsukawa, M. Sangermano, *ACS Appl. Polym. Mater.* **2024**, *6*, 2868.
[15] A. Medellin, W. Du, G. Miao, J. Zou, Z. Pei, C. Ma, *J Micro Nanomanuf.* **2019**, *7*, 031006.
[16] M. Bergoglio, Z. Najmi, A. Cochis, M. Miola, E. Vernè, M. Sangermano, *Polymers* **2023**, *15*, 4089.

[17] A. Truncali, I. Ribca, J. Yao, M. Hakkarainen, M. Johansson, *J. Appl. Polym. Sci.* **2023**, *140*, e54645.
[18] W. Xu, X. Wang, N. Sandler, S. Willför, C. Xu, *ACS Sustainable Chem. Eng.* **2018**, *6*, 5663.
[19] C. Noè, A. Cosola, C. TondaTuro, R. Sesana, C. Delprete, A. Chiappone, M. Hakkarainen, M. Sangermano, *Polymer* **2022**, *247*, 124779.
[20] T. M. Joseph, A. Kallingal, A. M. Suresh, D. K. Mahapatra, M. S. Hasanin, J. Haponiuk, S. Thomas, *Int. J. Adv. Manuf. Technol.* **2023**, *125*, 1015.
[21] M. Porcarello, C. Mendes-Felipe, S. Lanceros-Mendez, M. Sangermano, *Sustainable Mater. Technol.* **2024**, *40*, e00927.
[22] L. Pezzana, R. Wolff, G. Melilli, N. Guigo, N. Sbirrazzuoli, J. Stampfl, R. Liska, M. Sangermano, *Polymer* **2022**, *254*, 125097.
[23] L. Papadopoulos, L. Pezzana, N. M. Malitowski, M. Sangermano, D. N. Bikiaris, T. Robert, *ACS Omega* **2023**, *8*, 31009.
[24] A. L. Flourat, L. Pezzana, S. Belgacem, A. Dosso, M. Sangermano, S. Fadlallah, F. Allais, *Green Chem.* **2023**, *25*, 7571.
[25] L. Pezzana, R. Wolff, G. Melilli, N. Guigo, N. Sbirrazzuoli, J. Stampfl, R. Liska, M. Sangermano, *Polymer* **2022**, *254*, 125097.
[26] L. Papadopoulos, L. Pezzana, N. Malitowski, N. Kladovasilakis, D. Tzetzis, M. Sangermano, D. N. Bikiaris, T. Robert, *Giant* **2024**, *18*, 100275.
[27] R. Sesia, S. Ferraris, M. Sangermano, S. Spriano, *Polymers* **2022**, *14*, 4645.
[28] R. Sesia, A. G. Cardone, S. Ferraris, S. Spriano, M. Sangermano, *Prog. Org. Coat.* **2024**, *189*, 108311.
[29] H. El Gharras, *Int. J. Food Sci. Technol.* **2009**, *44*, 2512.
[30] A. Arbenz, L. Avérous, *Green Chem.* **2015**, *17*, 2626.
[31] A. Pizzi, *Biomolecules* **2019**, *9*, 344.
[32] A. K. Koopmann, C. Schuster, J. Torres-Rodríguez, S. Kain, H. Pertl-Obermeyer, A. Petutschnigg, N. Hüsing, *Molecules* **2020**, *25*, 4910.
[33] B. Yan, Z. S. Chen, Y. Hu, Q. Yong, *Front. Bioeng. Biotechnol.* **2021**, *9*, 753898.
[34] G. Riccucci, M. Cazzola, S. Ferraris, V. A. Gobbo, M. Miola, A. Bosso, G. Örlygsson, C. How Ng, E. Verné, S. Spriano, *J. Am. Ceram. Soc.* **2021**, *105*, 1697.
[35] C. Reggio, J. Barberi, S. Ferraris, S. Spriano, *Metals* **2023**, *13*, 1347.
[36] R. Sesia, S. Spriano, M. Sangermano, S. Ferraris, *Metals* **2023**, *13*, 1070.
[37] F. H. A. Fernandes, H. R. N. Salgado, *Crit. Rev. Anal. Chem.* **2016**, *46*, 257.
[38] I. Mueller-Harvey, *Anim. Feed Sci. Technol.* **2001**, *91*, 3.
[39] S. Ma, Y. Jiang, X. Liu, L. Fan, J. Zhu, *RSC Adv.* **2014**, *4*, 23036.
[40] C. Aouf, J. Lecomte, P. Villeneuve, E. Dubreucq, H. Fulcrand, *Green Chem.* **2012**, *14*, 2328.
[41] K. Tan, R. Liu, J. Luo, Y. Zhu, W. Wei, X. Liu, *Prog. Org. Coat.* **2019**, *130*, 214.
[42] L. Cao, X. Liu, H. Na, Y. Wu, W. Zheng, J. Zhu, *J. Mater. Chem. A Mater.* **2013**, *1*, 5081.
[43] X. Wang, J. Zhang, J. Liu, R. Liu, J. Luo, *Colloids Surf., A* **2022**, *644*, 128834.
[44] Y. Li, Z. Qu, K. Wu, P. Lv, H. Meng, H. Zheng, J. Shi, M. Lu, X. Huang, *Eur. Polym. J.* **2021**, *148*, 110358.
[45] A. A. Haroun, S. A. El Toumy, *J. Appl. Polym. Sci.* **2010**, *116*, 2825.
[46] G. Zhu, J. Zhang, J. Huang, X. Yu, J. Cheng, Q. Shang, Y. Hu, C. Liu, L. Hu, Y. Zhou, *Green Chem.* **2021**, *23*, 5911.
[47] A. W. C. van den Berg, U. Hanefeld, *J. Chem. Educ.* **2006**, *83*, 292.
[48] J. E. Cobb, C. M. Cribbs, B. R. Henke, D. E. Uehling, *Encyclopedia of Reagents for Organic Synthesis*, Wiley, Chichester, UK **2005**.
[49] R. S. Waritz, R. M. Brown, *Am. Ind. Hyg. Assoc. J.* **1975**, *36*, 452.
[50] J. Nordlund, P. Grimes, J. Ortonne, *J. Eur. Acad. Dermatol. Venereol.* **2006**, *20*, 781.
[51] F. J. Enguita, A. L. Leitão, *BioMed Res. Int.* **2013**, *2013*, 542168.
[52] D. Haldar, M. K. Purkait, *Chemosphere* **2021**, *264*, 128523.
[53] A.-M. Galan, I. Calinescu, A. Trifan, C. WinkworthSmith, M. CalvoCarrascal, C. Dodds, E. Binner, *Chem. Eng. Proc.* **2017**, *116*, 29.
[54] H. Li, Y. Qu, Y. Yang, S. Chang, J. Xu, *Bioresour. Technol.* **2016**, *199*, 34.
[55] A. Hoz, A. Diaz-Ortiz, A. Moreno, *Curr. Org. Chem.* **2004**, *8*, 903.
[56] N.-J. Hempel, M. M. Knopp, R. Berthelsen, K. Löbmann, *Molecules* **2020**, *25*, 1068.
[57] K. Martina, G. Cravotto, R. S. Varma, *J. Org. Chem.* **2021**, *86*, 13857.
[58] M. Zanon, A. Chiappone, N. Garino, M. Canta, F. Frascella, M. Hakkarainen, C. F. Pirri, M. Sangermano, *Mater. Adv.* **2022**, *3*, 514.
[59] J. Yao, M. Karlsson, M. Lawoko, K. Odelius, M. Hakkarainen, *RSC Sustainability* **2023**, *1*, 1211.
[60] J. Yao, K. Odelius, M. Hakkarainen, *ACS Appl. Polym. Mater.* **2021**, *3*, 3538.
[61] L. Pezzana, G. Melilli, P. Delliere, D. Moraru, N. Guigo, N. Sbirrazzuoli, M. Sangermano, *Prog. Org. Coat.* **2022**, *173*, 107203.
[62] M. D. Goodner, C. N. Bowman, *Macromolecules* **1999**, *32*, 6552.
[63] R. Ding, Y. Du, R. B. Goncalves, L. F. Francis, T. M. Reineke, *Polym. Chem.* **2019**, *10*, 1067.
[64] C. Vazquez-Martel, L. Becker, W. V. Liebig, P. Elsner, E. Blasco, *ACS Sustainable Chem. Eng.* **2021**, *9*, 16840.
[65] A. Liguori, S. Subramaniyan, J. G. Yao, M. Hakkarainen, *Eur. Polym. J.* **2022**, *178*, 111489.
[66] Y. Xu, K. Odelius, M. Hakkarainen, *ACS Sustainable Chem. Eng.* **2020**, *8*, 17272.
[67] J. F. Stanzione, III, J. M. Sadler, J. J. La Scala, K. H. Reno, R. P. Wool, *Green Chem.* **2012**, *14*, 2346.
[68] C. Zhang, S. A. Madbouly, M. R. Kessler, *Macromol. Chem. Phys.* **2015**, *216*, 1816.
[69] L. Pezzana, M. Sangermano, *Prog. Org. Coat.* **2021**, *157*, 106295.
[70] A. Cosola, A. Chiappone, M. Sangermano, *Mol. Syst. Des. Eng.* **2022**, *7*, 1093.
[71] C. Mendes-Felipe, I. Isusi, O. GómezJiménez-Aberasturi, S. Prieto-Fernandez, L. Ruiz-Rubio, M. Sangermano, J. L. VilasVilela, *Polymers* **2023**, *15*, 3136.

